Measurement of seismically induced pressure at the foundation-soil interface of a model bridge pier with plastic hinge development

Y. Chen, & T. Larkin

The University of Auckland, Auckland, New Zealand.

ABSTRACT: Recent studies have suggested that incorporating soil-foundation-structure-interaction (SFSI) may reduce the seismic design forces on a bridge superstructure thereby avoiding extensive damage. However, most previous investigations, especially experimental research, focus on the structural behaviour and seldom address the response of the foundation. In this paper, the effects of SFSI on the response of a scaled bridge pier supported on sand are considered utilising shake table testing. A laminar box allows an improved approximation to the seismically induced shear deformation of the sand in situ. With the implementation of a pressure mapping system, the contact pressure at the foundation-soil interface is measured during the dynamic response. Thus, the time history of pressure on the foundation/sand interface from vertical and rotational loading is quantified and yielding of the supporting soil is evident when it occurs. An artificial plastic hinge is constructed at the base of the bridge column to simulate irrecoverable deformation of the structure should it develop. Therefore, the effect on nonlinear soil behaviour on plastic hinge development can be measured.

1 INTRODUCTION

Structures with strong soil-foundation-structure interaction (SFSI) have been found to perform very well under strong earthquakes. In the 2010 Darfield earthquake, the spectral acceleration of recorded ground motion was significantly higher than the prescribed values in the New Zealand design standard, NZS 1170.5 (Bradley, 2012). Some structures on shallow foundations only experienced minor damage in this event. Through numerical simulation Storie et al. (2014) concluded that this was due to SFSI. A large portion of the seismic energy was dissipated via plastic deformation of supporting soil and uplift of the foundation.

The effect of soil was incorporated in numerical modelling by Yim and Chopra (1984) using a Winkler model, by Wolf (1994) using a cone model and by Paulucci et al. (2008) using macro-element models. The results from these analyses also showed that rocking of shallow foundations can be an effective mechanism of seismic isolation, thus bringing benefit to the structure.

Several experimental investigations on structures with SFSI have been conducted. Shirato et al. (2008) conducted a series of shake table and cyclic tests on a structure-foundation system. The results from the experiments were used to verify the macro-element model of Paulucci et al. (2008). Drosos et al. (2012) also carried out a set of shake table tests using sinusoidal excitations. The results showed that a decrease of foundation width could increase the accumulated settlement. However, in these studies flexibility of the structure and possible plastic hinge development of the column were not taken into account. Deng et al. (2012) performed a group of centrifuge tests on a simplified bridge model using notches to simulate a plastic hinge. Qin et al. (2013) conducted several shake table tests on a single-degree of freedom structure with an artificial plastic hinge. The test results showed that SFSI was beneficial into reducing the unrecoverable deformation of the structure. Although these experimental investigations have considered the effect of plastic hinge development, the loading on foundation in these studies has not be measured and discussed.

In this study, using a pressure mapping system, the vertical and rotational loading on the soil-foundation interface was recorded. Thus, yielding of the surface soil was evident. The effect of column plastic hinge development on the nonlinear soil behaviour was revealed. The findings of this study provide a means to an understanding on the seismic loading on a bridge foundation with consideration

of both nonlinearities of structure and supporting soil, which to the authors' knowledge is the first time physical modelling of this complexity has been studied.

2 METHODOLOGY

2.1 *Sand deposition and properties*

The dry sand used throughout the tests was an industrially produced clean quartz material. It was classified as a fine uniform sand with uniformity coefficient C_u = 1.9. In accordance with NZS 4402.4 (1997), laboratory tests showed that the sand had maximum and minimum densities of 14.2 and 17.2 kN/ m^3, respectively. The sand was rained from a height of 0.9 m above the shake table through the floor of a box containing holes at constant spacing, until a depth of 400 mm of sand was achieved. The container was a laminar box constructed to approximately simulate seismic shear wave deformation of the sand in situ by Cheung et al. (2013). To ensure the density of the sand was consistent spatially, samples were taken during raining of the sand at various locations in the laminar box. The dry density was measured to be between 15.2 to 15.4 kN/m^3, i.e. a relative density (D_r) of 35%. The friction angle determined by drained triaxial tests was 37º.

2.2 *Experimental modelling*

The idealized bridge pier prototype was designed to have a shallow, rectangular foundation. The prototype, as schematically illustrated in Figure 1(a), consisted of a 121.5 tonne mass at the top, supported by a 9 m height reinforced concrete column with EI = 7807x10^6 kN/m^2. This resulted in a fixed-base fundamental frequency (f_p) of 2.59 Hz. The footing of the pier was designed using Verification Method B1/VM4 in the New Zealand Building Code (DBH, 2011) for shallow foundations. The initial properties of sand deposited into the laminar box were utilized in the design of the foundation, i.e. γ = 15.3 kN/m3 and ϕ = 37º. The footing was design to sustain the ground excitation recorded on soil class D (soft soil) in an earthquake with 1000 year return period according to NZS 1170.5 (2004). The adopted dimensions were 8.4 m long by 2.25 m wide by 1.3 m thick. The vertical load due to self-weight of the pier-foundation system was equal to the ultimate vertical capacity of the underlying soil under seismic load.

The prototype was represented as a single-degree of freedom system and downscaled using the principles of similitude, according to the single gravity modelling method outlined in Muir Wood (2004). A linear geometric scale of n = 1/15 was selected. The scale factors are shown in Table 1.

The experimental model was constructed from steel (Figure 1 (b)) and has a fixed-base natural frequency (f_m) of 10 Hz. A dynamic analysis of the model footing indicated that the ultimate vertical capacity was equal to approximately 40% the weight of the model. Yielding of soil is thus more likely to occur in the model than in the prototype. Therefore, the results are presented in model scale. The ultimate capacity of the model foundation on sand of 4907 N was estimated according to Equation (1) modified from Terzaghi (1943) including the effect of uplift. The footing is assumed to be entirely in contact with the supporting soil, i.e. a = 1.

$$V_u = \frac{\gamma B^2 a L N_\gamma}{2}\left(1 - 0.3\frac{B}{aL}\right) \tag{1}$$

$$N_\gamma = 2(N_q - 1)\tan\phi \text{ and } N_q = e^{\pi\tan\phi}\tan^2(45 + \phi/2)$$

where B = 0.14 m and L = 0.56 m are the width and length of the footing, respectively.

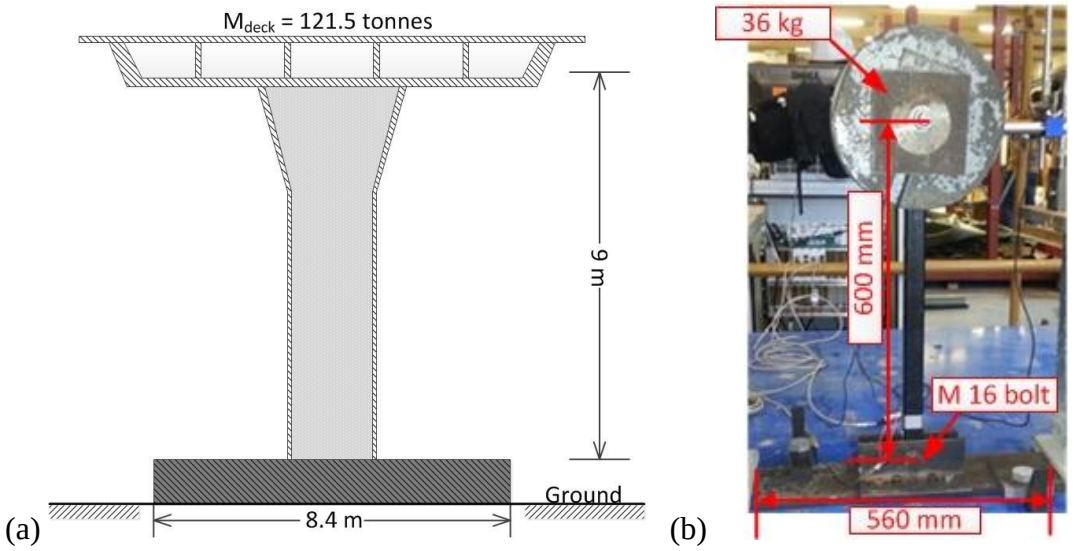

Figure 1. (a) Prototype and (b) experimental model

Table 1. Scale factors applied

Quantity	Scale factor
Length	S_L = 15
Mass	$S_m = {S_L}^3$ = 3375
Accelerations	S_a = 1
Time	$S_t = \sqrt{S_L/S_a}$ = 3.873
Lateral Stiffness	$S_k = (S_a * S_m)/S_L$ =225

2.3 *Ground excitation*

The ground motion applied herein was the fault-parallel component at Bolu station recorded in 1999 Duze earthquake, Turkey (PEER, 2014). It was classified as a near-fault ground motion with a strong acceleration pulse by Shahi and Baker (2014). The excitation applied was scaled to fit the design spectrum (at 10 Hz) specified in NZS1170.5:2004 for subsoil class D, in Christchurch with a return period of 1000 years. The applied excitation and response spectrum are shown in Figure 2. The strong acceleration pulse is highlighted in Figure 2(a).

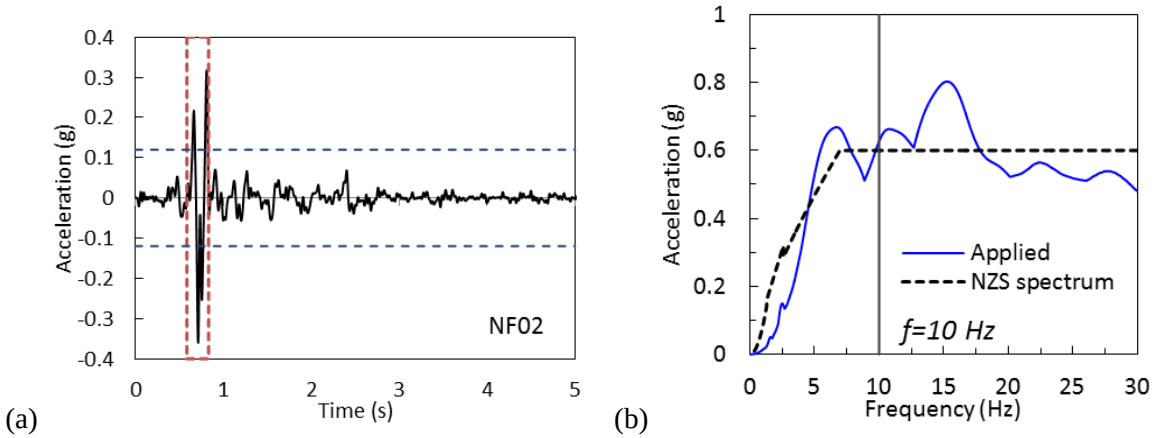

Figure 2. (a) Ground motion applied and (b) its response spectrum

2.4 *Artificial plastic hinge of the bridge column*

In small scale testing it is difficult to scale the flexural capacity of bridge column using material nonlinearity. Therefore, to simulate any structural damage, an artificial plastic hinge was constructed at the base of the column using an M16 bolt (Figure 1(b)). A similar method was used by Qin et al. (2013). The bolted hinge connects the column and the foundation of the model. Once the bending moment at the column base exceeds the pre-set capacity of the hinge, rotational slippage takes place. Thus, unrecoverable deformation of the structure is able to be simulated. A torque wrench was used to ensure a consistent pre-set capacity of the connection throughout the tests. A series of push-over tests on the model fixed at the base with varying hinge capacity were conducted to define the capacity of the hinge. The results showed that friction of the connection has negligible effect on the elastic limit of the hinge.

According to the response spectra of ground motion applied (Figure 2(b)), the maximum bending moment at the base of the column with a fixed-base assumption was approximately 127 Nm. Thus, a hinge capacity of 160 Nm (torque wrench reading of 240 Nm) was utilised to simulate an elastic bridge column under the target seismic loading.

Figure 3 shows the cross-section of the theoretical bearing strength surface of the model footing based on Equation (2) (EC 7, 2001). Plastic deformation occurs once the combined loads exceed the bearing strength surface. Uplift is assumed to take place and the maximum separation between the footing and soil is assumed to be 60%, i.e. a = 0.6.

$$f(\overline{V},\overline{H},\overline{M}) = \overline{V} - (1-\frac{2|\overline{M}|}{\overline{V}})^2(1-\frac{|\overline{H}|}{\overline{V}})^3 = 0 \qquad (2)$$

where $\overline{V} = \frac{V}{V_{u,a=0.6}}$, $\overline{H} = \frac{H}{V_{u,a=0.6}}, \overline{M} = \frac{M}{V_{u,a=0.6}L}$ and V is the self-weight of the model, H and $M = 0.6H$ are the base shear and overturning moment. Bearing failure of the underlying soil is predicted to occur when the overturning moment reaches 64.5 Nm. Therefore, a low hinge capacity of 70 Nm with torque wrench reading of 100 Nm was applied to simulate the possible plastic hinging of the bridge column.

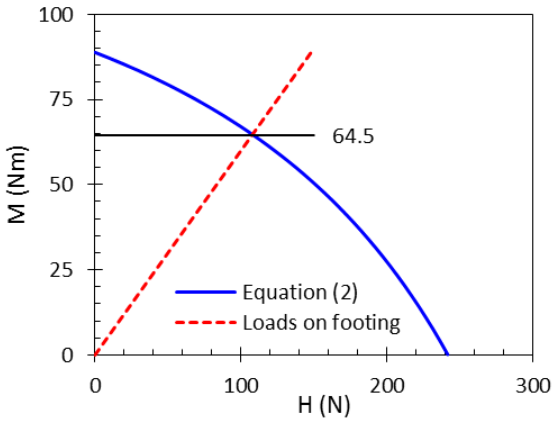

Figure 3. Base shear and corresponding overturning moment to mobilise failure of the model foundation

2.5 *Setup and instrumentations*

The shake table testing was performed for two support conditions: (1) fixed on a rigid base and (2) the SFSI case, i.e. free to uplift when supported on a base of sand. The fixed base assumption was simulated by fixing the foundation of the model to the shake table using clamps. For the second supporting condition the clamps were removed and the model was placed on the surface of the sand contained in the laminar box, which was then placed on the shake table. The setup for the SFSI test is shown in Figure 4(a). The sand was rained into the laminar box, in a controlled manner to ensure reasonable uniformity, at the beginning of testing. The pier-footing model was instrumented to allow

direct recording of accelerations, column strains, displacements and loads. The pressure distribution at the foundation-soil interface was recorded using a tactile pressure mapping system (Figure 4(b)). The authors recognise that placing a pressure mat in the experimental system has the potential to create inaccuracies through compliance, however, the accuracy of this system to reliably measure normal pressure was confirmed by Palmer et al. (2009). For the model footing of 560 x 140 mm, a matrix of 7x30 sensor points of the map was utilised. A sensor measures the pressure of a surrounding 18.75x18.75 mm area. Thus, vertical force at a sensor point can be calculated as the product of the recorded pressure and the contributing area (352 mm^2). The resultant vertical load at the base of footing, *V*, was estimated as the summation of the vertical forces. The moment, *M*, was estimated by taking the summation of the products of the vertical force and the distance between the sensor and the centre of the footing. The horizontal load, *H*, was assumed to be equal to the base shear of the structure and estimated by the product of acceleration of the mass and the mass itself was 36 kg.

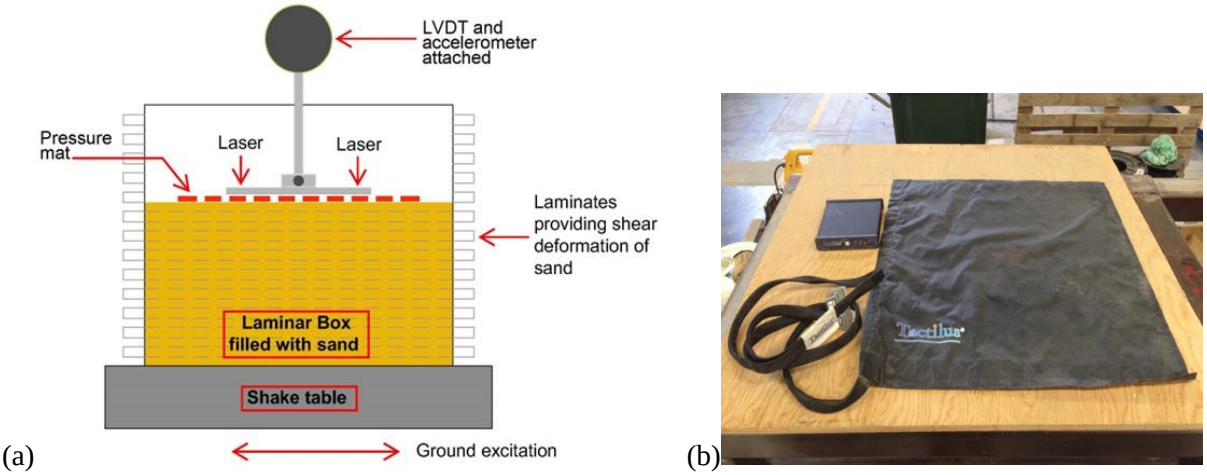

Figure 4. (a) Experimental setup for the model with SFSI and (b) pressure mat

3 RESULTS AND DISCUSSION

3.1 *Effect of plastic hinge development on the foundation pressure distribution*

As shown in Figure 5, the maximum moment on the footing occurred during the strong acceleration pulse. This is because nearly all of the seismic energy of a near-fault pulse-like ground motion is released via the pulse. When the plastic hinge at the column base was activated, the maximum moment acting on the footing was less than that of an elastic structure. The maximum moment of the elastic structure occurred at 0.89 s, which was later than that of the case involving a plastic hinge. The minimum contact area (*a*) at the footing-soil interface took place at the time of the maximum moment in both cases. Figure 5 shows footing uplift is more significant in the case of no plastic hinge. The contact pressure distribution at the time of maximum separation of the footing and the supporting sand is also shown in Figure 5. It can be seen that the footing of the elastic structure was under a higher contact pressure compared to the case where plastic hinge development occurred. The results suggest that the stronger the moment on the footing, the larger the separation between the footing and its support leading to a larger contact pressure. The figure also indicates that plastic hinge development took place at 0.81 s and significantly reduced the moment on the footing that resulted from the following load reversal at 0.89 s.

3.2 *Effect of plastic hinge development on yielding of the supporting soil*

The theoretical bearing yield surface of the supporting soil, simulated using Equation (2), is plotted in Figure 6. The value of *a* in Equation 2 is taken to be the minimum contact area shown in Figure 5. If the combined load of base shear and moment on the footing is within the theoretical bearing surface, the soil beneath the footing is predicted to behave elastically. Once the combined load reaches or exceeds the bearing surface, the supporting soil is considered to experience plastic deformation. Evidence of yielding of the supporting soil is shown in the case of no plastic hinge development but

not in the case of development of a plastic hinge. Four data points from the shake table tests were found to exceed the theoretical surface modelled by Equation (2) in Figure 6(a), while no such data is shown in Figure 6(b). As a result of the low bearing capacity of the supporting soil, due to a low state of effective stress, yielding of the soil is more likely to occur in the case of the elastic structure since the moment is the larger of the two cases.

The temporal size of the theoretical bearing surface, $f(\bar{V}, \bar{H}(t), \bar{M}(t))$, was calculated from Equation (2) with the instantaneous observed loads and contact area, $H(t)$, $M(t)$ and $a(t)$. When $f(\bar{V}, \bar{H}(t), \bar{M}(t))$ (denoted as $f(t)$ in Figure 7) is greater than or equal to zero, yielding of the supporting soil is predicted. As shown in Figure 7(a), without plastic hinge development in the structural column, yielding of supporting soil took place twice, i.e. at 0.8 and 0.9 s. However, with the development of a plastic hinge, yielding of soil did not theoretically occur.

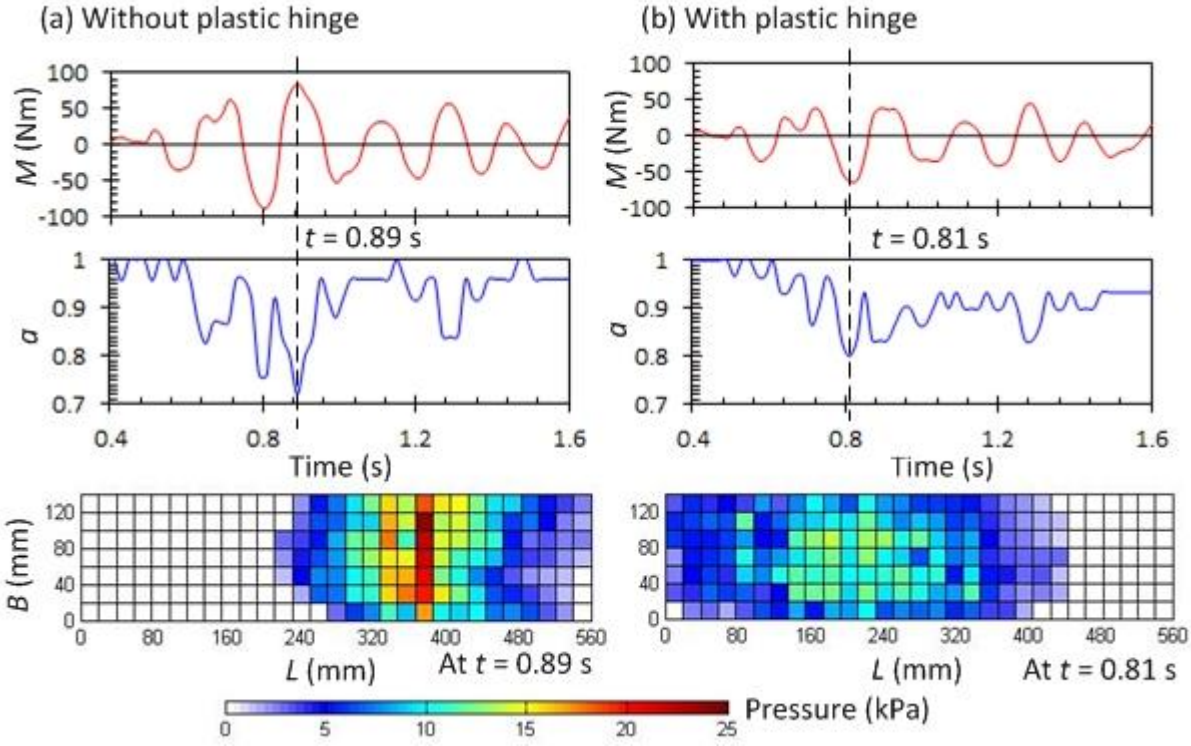

Figure 5. Contact area, moment and contact pressure at the time of minimum contact

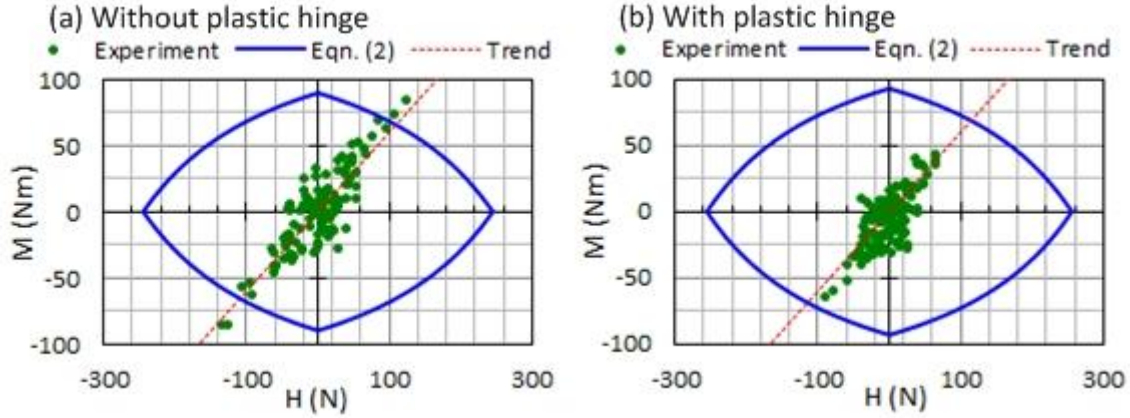

Figure 6. Projection of observed forces and theoretical failure surface in *H-M* plane

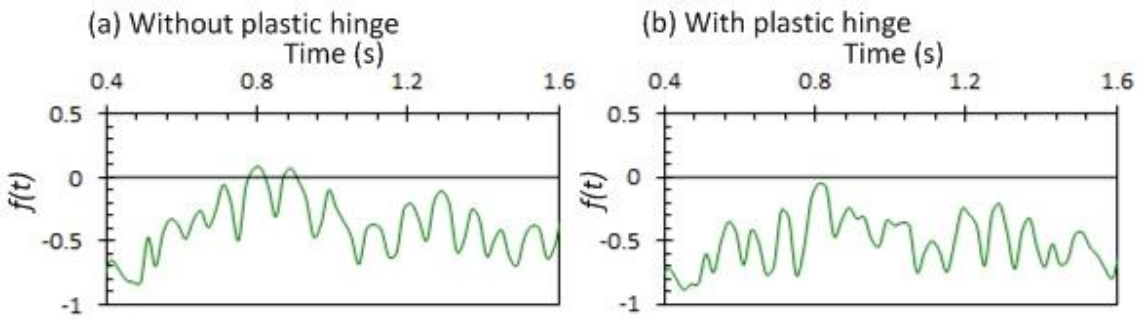

Figure 7. Position of instantaneous observed loads regarding to the failure surface

3.3 *Interaction of structural plastic hinge development and nonlinear soil deformation*

When the model is fixed on a rigid base, i.e. without SFSI, the maximum total displacement is equal to the maximum rotation of the hinge times the height to the centre of mass of the structure. When the potential hinge at the column base is tighten to a torque of 240Nm no hinge rotation is possible with the motions induced in these tests. In this case when the structure is placed on the surface of the sand, i.e. SFSI can occur, the maximum displacement of the mass is equal to the product of the maximum footing rotation and structural height, neglecting the very small displacement from structural distortion of the column. The displacement at the top of structure with the interaction of these two nonlinearities is the sum of displacement induced by both the plastic hinge development and the footing rotation due to SFSI. In the case studied herein, the maximum displacement resulting from SFSI only is approximately three times of that from plastic hinge development only. The substantial deformation in the case with SFSI only is due to deformation of loose sand without compaction. With the interaction of both nonlinearities, less deformation of the structure and soil were observed compared to the cases of only a single nonlinearity.

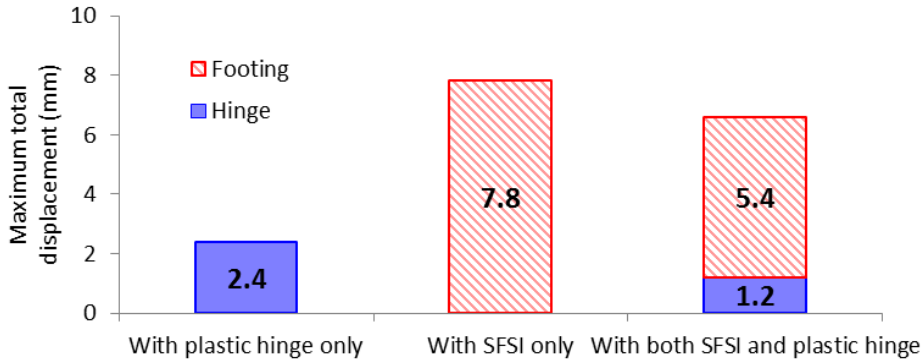

Figure 8. Effect of SFSI and plastic hinge development on the maximum total displacement (top of mass)

4 CONCLUSIONS

In this study, shake table tests on a scaled bridge pier with both SFSI and plastic hinge development in the column are reported. SFSI was incorporated by placing the model on loose sand in a laminar box and structural plastic hinge development was simulated by a bolted connection (torqued to allow rotational displacement) at the base of column. The contact pressure at the footing-soil interface was recorded utilising a pressure mapping sensor. From this recorded data, the areas of separation were identified and moments on the footing were calculated. The combined load on the footing was compared with the theoretical bearing surface suggested by Eurocode 7 (2001). The results reveal that:

- Plastic hinge development in the bridge column reduces the maximum moment on the footing, causes a smaller minimum contact area at the footing-soil interface and a larger maximum contact pressure than those in the case of the elastic structure.
- Yielding of the supporting soil is more likely to occur in the case of an elastic structure where no plastic hinge development occurs.

- The interaction of simultaneous plastic hinge development and SFSI reduces the contribution of each nonlinearity, to the horizontal displacement of the structure, from that when acting alone.

ACKNOWLEDGEMENTS:

The research is funded by the Ministry of Business, Innovation and Employment through the Natural Hazards Research Platform under the Award UoA 3701868.

REFERENCES:

Bradley, B. A. 2012. Strong ground motion characteristics observed in the 4 September 2010 Darfield, New Zealand earthquake. *Soil Dynamics and Earthquake Engineering*, 42, 32-46.

Cheung, W.M., Qin, X., Chouw, N. Larkin, T. and Orense R. 2013. Experimental and numerical study of soil response in a laminar box. *New Zealand Society for Earthquake Engineering Annual Conference, 2013*, Wellington, New Zealand.

DBH. 2011. *Compliance Document for the New Zealand Building Code - Clause B1 Structure*, Department of Building and Housing, Wellington, New Zealand.

Deng, L. and Kutter, B.L. 2012. Characterization of rocking shallow foundations using centrifuge model tests. *Earthquake Engineering and Structural Dynamics*, 41 (5), 1043-1060.

Drosos, V., Georgarakos, T., Loli, M., Anastasopoulos, I., Zarzouras, O., and Gazetas, G. 2012. Soil-foundation-structure interaction with mobilization of bearing capacity: experimental study on sand. *Journal of Geotechnical and Geoenvironmental Engineering*, ASCE, 138, 1369-1386.

EC7 Drafting Committee. (2001), *Eurocode 7: Part 1: Geotechnical Design, General Rules*. European Committee for Standardization. Brussels.

Muir, Wood, D. 2004. *Geotechnical Modelling*, Spon Press, London.

NZS 1170.5. 2004. *Structural Design Action, Part 5: Earthquake Actions.* Standards New Zealand, Wellington, New Zealand. ISBN 1-86975-018-7.

NZS 4402.4.2. 1997. *Determination of the Minimum and Maximum Dry Densities and Relative Density of a Cohesionless Soil*. Standards New Zealand, Wellington, New Zealand. ISBN 1-86975-018-5.

Pacific Earthquake Engineering Research Center (PEER). 2014. Next generation attenuation database, http://peer.berkeley.edu/peer_ground_motion_database.

Palmer, M.C., O'Rourke, T.D., Olson, N.A., Abdoun, T., Ha, D. and O'Rourke M.J. 2009. Tactile pressure sensors for soil-structure interaction assessment. *Journal of Geotechnical and Geoenvironmental Engineering*, 135(11), 1638-1645.

Paolucci, R., Shirato, M., and Yilmaz, M. T. 2008. Seismic behaviour of shallow foundations: Shaking table experiments vs numerical modelling. *Earthquake Engineering and Structural Dynamics*, 37(4), 577-595.

Qin, X., Chen, Y. and Chouw, N. 2013. Effect of uplift and soil non-linearity on plastic hinge development and induced vibrations in structures. *Advances in Structural Engineering*, 16(1), 153-147.

Shahi, S. K., and Baker, J. W. 2014. An efficient algorithm to identify strong velocity pulses in multicomponent ground motions. *Bulletin of the Seismological Society of America*, 104(5), 2456-2466.

Shirato, M., Kouno, T., Asai, R., Nakatani, S., Fukui, J., and Paolucci, R. 2008. Large-scale experiments on nonlinear behaviour of shallow foundations subjected to strong earthquakes. *Soils and Foundations*, 48(5), 673-692.

Storie, L.B., Pender, M.J., Clifton, G.C. and Wotherspoon, L.M. 2014. Soil-foundation-structure-interaction for buildings on shallow foundations in the Christchurch earthquake. *10th US National Conference of Earthquake Engineering 2014*, Anchorage, Alaska.

Terzaghi, K. 1943. *Theoretical Soil Mechanics*, Wiley.

Wolf, JP. 1994. *Foundation Vibration Analysis Using Simple Physical Models*. Englewood Cliffs, NJ: Prentice-Hall.

Yim, C. S., and Chopra, A. K. 1984. Earthquake response of structures with partial uplift on Winkler foundation. *Earthquake Engineering and Structural Dynamics*, 12(2), 263-281.